Catalysis Letters
https://doi.org/10.1007/s10562-020-03103-4

Amine Functionalized Graphene Oxide Stabilized Pickering Emulsion for Highly Efficient Knoevenagel Condensation in Aqueous Medium

Jie Zhu[1] · **Fei Wang**[1] · **Dongsheng Li**[1] · **Jie Zhai**[1] · **Ping Liu**[1] · **Weihong Zhang**[1] · **Yongxin Li**[1]

Received: 23 August 2019 / Accepted: 9 January 2020

Abstract

A Pickering emulsion catalytic system was developed using amphiphilic amine-functionalized graphene oxide (GO-NH_2) for a Knoevenagel condensation in aqueous medium instead of organic solvent. The properties of GO-NH_2 and the Pickering emulsion stabilized by GO-NH_2 were characterized by Fourier-transform infrared (FT-IR) spectroscopy, thermogravimetric analysis (TGA), X-ray diffraction (XRD) analysis, X-ray photoelectron spectroscopy (XPS), organic elemental analysis (OEA), contact angle (CA), Brunauer–Emmett–Teller surface area, and optical microscopy. The results indicated that the properties of the as-prepared Pickering emulsion system, such as droplet density, size, and distribution, were greatly affected by the amount of GO-NH_2 and the oil–water ratio, which were closely related to the catalytic performance for Knoevenagel condensation reactions. Furthermore, this Pickering emulsion system for the Knoevenagel condensation in an aqueous medium exhibited a much higher catalytic activity than those of GO-NH_2 in organic solvents under the same reaction conditions. The reaction rate constant (*k*) in the Pickering emulsion system was calculated to be 0.043 min^{-1} at 50 °C. The enhanced activity of the Pickering emulsion was mainly attributed to large interfaces between GO-NH_2 and reactants in the emulsion, and the clear confinement effect. Furthermore, GO-NH_2 remained stable for preparing Pickering emulsion systems after recycling in six runs, exhibiting its good reusability.

Graphic Abstract

A novel Pickering emulsion catalytic system was developed using amphiphilic amine functionalized graphene oxide (GO-NH2) for Knoevenagel condensation in aqueous medium instead of organic solvents. It exhibited excellent catalytic performance in the reaction.

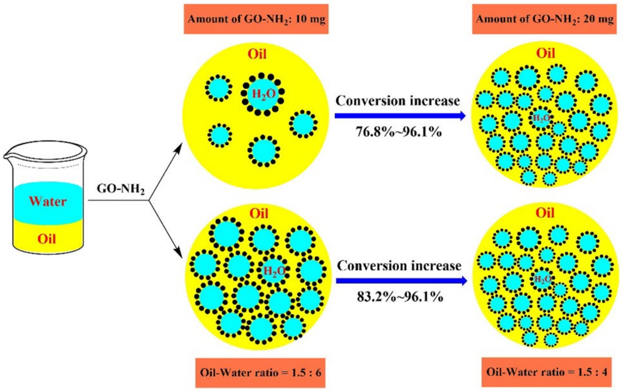

Keywords Pickering emulsion · Graphene oxide · Amine functionalization · Knoevenagel condensation

---

Electronic supplementary material The online version of this article (https://doi.org/10.1007/s10562-020-03103-4) contains supplementary material, which is available to authorized users.

Extended author information available on the last page of the article

1 Introduction

The Knoevenagel condensation is an important reaction for forming carbon–carbon double bonds (C=C). The resulting α,β-unsaturated carbonyl compounds are valuable intermediates in the pharmaceutical, cosmetic, and pesticide industries [1–3]. Generally, the Knoevenagel condensation occurs in the presence of base catalysts, such as organic amines and piperidine [4, 5]. Despite the high catalytic activity of these catalysts, the required separation of products and catalysts, and catalyst recovery, owing to their inherently homogeneous nature, limits their applications in industrial production [6, 7]. Therefore, organic amines can be grafted on solid particles (such as polymers, zeolites, and silica) to serve as heterogeneous catalysts for this reaction [8–11].

The Knoevenagel condensation traditionally proceeds in organic solvents [12–14]. Therefore, some disadvantages of organic solvents, such as high cost and environment pollution, restrict their further practical applications [15]. In comparison, water, as a green solvent, has received increasing interest recently in catalysis and organic synthesis. Unfortunately, most weakly polar reactants are poorly soluble in water, which can produce serious mass transfer limitations in aqueous–organic biphasic systems. Performing the Knoevenagel condensation in aqueous medium is clearly unfavorable owing to the weakly polar nature of the reactants, namely, benzaldehyde (BAL) and its derivatives.

Recently, Pickering emulsions stabilized by amphiphilic solid particles have attracted much attention owing to their innovative applications in designing efficient two-liquid-phase catalytic systems [16–19]. Pickering emulsions can greatly decrease mass transfer limitations in a reaction by enlarging the interfaces between catalysts and reactants, obtaining high catalytic activities. To achieve this objective, some solid particles (such as silica and zeolites) are often functionalized by grafting with some moieties to construct amphiphilic surfaces. For example, Zapata et al. [20] synthesized interface-active zeolites by grafting organosilanes on the surface of HY zeolites. The resulting emulsions stabilized by interface-active zeolites can significantly improve catalytic efficiency in biofuel upgrading reactions in water/oil biphasic systems.

Presently, graphene oxide (GO) is often employed as a promising catalyst support. Compared with traditional supports (such as silica and zeolites), GO has several significant advantages, including high hydrothermal stability, strong resistance to acid and base, good electronic transfer properties, and minimal mass transfer limitations [21, 22]. More importantly, GO and its derivatives (such as amine-functionalized GO in this study) have been shown in previous studies to possess predominant amphiphilic properties. This favors the formation of a Pickering emulsion in two-liquid-phase systems, resulting in high catalytic activities [23, 24]. For example, He et al. [25] reported the preparation of a stable Pickering emulsion, employing GO and GO-supported Ag (Ag/GO) as emulsifiers. The Ag/GO-stabilized emulsion exhibited good catalytic performance for the reduction of 4-nitrophenol.

Herein, we have successfully developed a Pickering emulsion system prepared from amine-functionalized graphene oxide (GO-NH_2) for catalysis of the Knoevenagel condensation for the first time. This Pickering emulsion greatly enlarged the interfaces between catalyst GO-NH_2 and the reactants, resulting in a small mass transfer limitation in the reaction and, therefore, high catalytic activity. The Pickering emulsion system stabilized by GO-NH_2 provided a highly efficient and environmentally friendly catalytic system for aqueous Knoevenagel condensation.

2 Experimental

2.1 Preparation of GO-NH_2 Catalyst

Graphene oxide was first prepared by the modified Hummers method [26]. GO (0.2 g) was then dispersed in DMSO (100 mL) and 3-aminopropyltrimethoxysilane (APTMS; 2.0 g) was added dropwise, followed by ultrasonication for 30 min three times. The mixture was then refluxed at 100 °C for 24 h. At the end of the grafting reaction, as-synthesized GO-NH_2 was collected by filtration and rinsed with absolute ethanol three times at room temperature to remove unreacted impurities. Finally, GO-NH_2 was dried under vacuum at 80 °C overnight.

The preparation process of GO-NH_2 was shown in Scheme 1. In addition, APTMS was grafted on SBA-15,

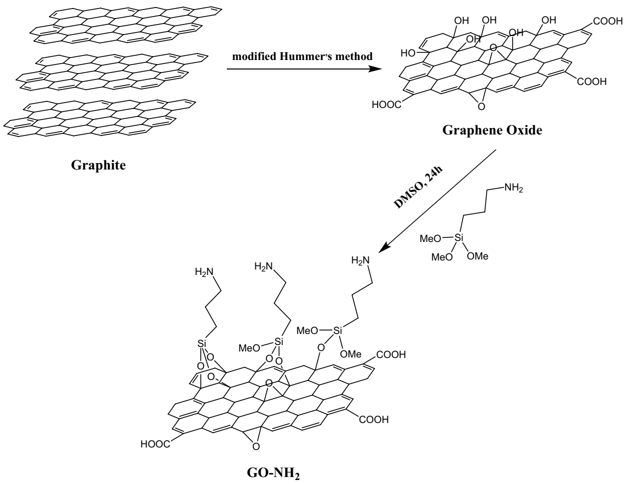

Scheme 1 Preparation process of GO-NH_2

using the same process as GO-NH_2. The resulting composite was named SBA-15-NH_2.

2.2 Catalytic Performance of Pickering Emulsion System on Knoevenagel Condensation

2.2.1 Preparation of Pickering Emulsion

Catalyst GO-NH_2 (10–25 mg), water (3–6 mL), and benzaldehyde (approximately 1.5 mL, 15 mmol) were successively added to a 50-mL round-bottom flask, followed by ultrasonication for 5 min. The mixture was then vigorously stirred at 800 rpm for 5 min to obtain the Pickering emulsion.

2.2.2 Knoevenagel Condensation

Knoevenagel condensation in this study (Scheme 2) was carried out in a 50 mL round-bottom flask.

Malononitrile (approximately 0.99 g, 15 mmol) and *n*-dodecane (internal standard substance, 0.3 mL) were successively added dropwise to the prepared Pickering emulsion. The reaction proceeded at 50 °C for 1 h. After the reaction was complete, the products were extracted with chloroform, followed by centrifugation to remove the catalyst and water. The reaction sample was analyzed by gas chromatography (SP-6850) equipped with a flame-ionization detector (FID) and a capillary column (SE-54) using nitrogen as the carrier gas. BAL conversion (*X*) and selectivity to benzalmalononitrile (BMA) were calculated through Eqs. (1), (2).

$$X = \frac{C_{BAL}^{0} - C_{BAL}}{C_{BAL}^{0}} \times 100\% \tag{1}$$

$$S_i = \frac{C_{BMA}}{C_{BAL}^{0} - C_{BAL}} \times 100\% \tag{2}$$

where C_{BAL} and C_{BMA} are the instant molar concentration of the reactant BAL and the product BMA in the reaction; $C^{0}{}_{BAL}$ is the initial molar concentration of BAL. The mass balance was close to or even better than 97%.

In addition, SBA-15-NH_2 was employed in Knoevenagel condensation for comparison.

2.2.3 Recovery of GO-NH_2

The recycled GO-NH_2 was filtered and rinsed with pure ethanol for three times at the room temperature, followed by drying under vacuum at 80 °C overnight.

2.3 Characterization of GO-NH_2 and Pickering Emulsion

Fourier-transform infrared (FT-IR) spectra of GO-NH_2were obtained using a Bruker TENSOR 27 spectrometer (Germany). Thermogravimetric analysis (TGA) was performed at room temperature to 650 °C with a heating rate of 20 $°C{\cdot}min^{-1}$ under nitrogen using a Perkin-Elmer TGA7 analyzer. The crystal composition of the sample was analyzed using a D/Max 2500PC X-ray diffractometer. (OEA) was performed using Thermo Scientific™ FLASH 2000 CHNS/O. The content of C, H and N elements in the sample could be accurately determined by the method of high temperature combustion. Contact angle tests were conducted using a DSA25 optical contact angle measuring device. Nitrogen adsorption–desorption isotherms were measured at – 196 °C using a TriStar3020 sorptometer (Micromeritics). The specific surface areas were calculated according to the Brunauer-Emmet-Teller (BET) method using adsorption data at relative pressure (p/p^o) in the range of 0.05–0.30. Morphologies of emulsions were characterized using an XSP-8CAE optical microscope (Shanghai Bim Co., Ltd).

2.4 Methodology of Processing XPS Data

X-ray photoelectron spectroscopy (XPS) measurements were performed using a Mulfilab 2000 spectrometer working in the constant analyzer energy mode with Al Kα radiation as the excitation source. The carbonaceous C 1 s line (284.6 eV) was used as the reference to calibrate the binding energies (B.E.).

2.4.1 Quantitative XPS Peak Analysis

Background removal methods have been proposed and used in the literature [27]. The Shirley background subtraction is one of the most widely used and was adopted in this study. To measure the area of spectral peaks correctly, the energy range of the spectrum (Emax and Emin) needs to be determined and fixed in a manner consistent for comparing different spectra of the same element. The tools of this study, including a graphical

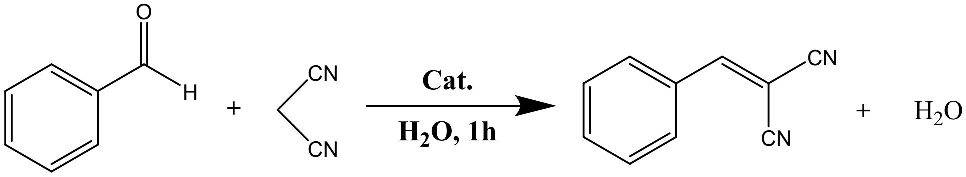

Scheme 2 Knoevenagel condensation between benzaldehyde and malononitrile

interface facilitating preview, were built with the MATLAB software from Math Works. The analysis consisted of a manual or automatic binding energy scale correction to remove the possible charging effect, a normalization to take differences in spectrometer response with time into account, a splitting of peaks and background if necessary and the multivariate procedure in itself.

2.4.2 Binding Energy Scale Correction

Insulating samples such as organic surfaces undergo positive charging when exposed to X-ray radiation, and as a result, the energy scale is shifted. Peak fitting of XPS spectra was performed using commercially available software, ESCA tools developed by Surface/Interface Inc. Binding energy scales are usually corrected using a reference peak of known binding energy (e.g., C–OH component of C 1*s* peak of contamination carbon) [27].

3 Results and Discussion

3.1 Characterizations of Synthesized GO-NH_2

The FT-IR spectra in Fig. 1 identified some functional groups on GO and GO-NH_2. Specifically, the FT-IR spectrum of GO (Fig. 1a) exhibited typical groups including carbonyl groups (C=O, 1724 cm^{-1}), *sp*^{2} carbon rings (C=C, 1616 cm^{-1}), epoxy groups (C–O–C, 1259 cm^{-1}), and hydroxyl groups (C–OH, 1068 cm^{-1}), in accordance with previous reports [20, 21, 28]. After grafting APTMS onto the GO surface, the spectrum of the sample showed distinct peaks for amino groups (C–NH_2) at 1569 and 773 cm^{-1}, corresponding to the stretching and wagging vibrations of N–H bonds, respectively [29, 30] (Fig. 1b), which clearly originated from APTMS. Notably, the appearance of a C–O–Si peak (1120 cm^{-1}) and a weaker C–OH peak (1068 cm^{-1}) hinted that APTMS was grafted to GO through covalent linkage via C–O–Si bonds [20]. In addition, the peak at 1650 cm-1 corresponding to the stretching vibration of amide group [29] was found in FT-IR spectrum of GO-NH2. It was attributed to the possible covalent combination of amino groups (–NH2) on APTMS with carboxyl groups (COOH) on GO in the process of grafting. Therefore, FT-IR results provided the direct evidence for the successful immobilization of APTMS on GO.

TGA of GO and GO-NH_2 was conducted to determine their thermal stability. The TG curve of GO (Fig. 2a) showed two significant weight losses before 250 °C. The first, below 125 °C, was derived from the evaporation of adsorbed water on GO. The second was found in the temperature range of 190–250 °C, accounting for approximately 25% of the total weight. This was reasonably attributed to the thermolysis of labile oxygen-containing functional groups (such as OH, C=O, and C–O–C) on GO. Continued weight loss was observed above 250 °C owing to thermolysis of the carbon skeleton [31]. The final weight loss was approximately 64% at 650 °C. In comparison, GO-NH_2 (Fig. 2b) showed gradual weight loss throughout the temperature range. The overall weight loss at 650 °C was approximately 41%, which was less than that of GO. Although APTMS was thermally unstable, the grafted APTMS on GO exhibits the higher thermal stability than GO in some temperature range due to the formation of stable C–O–Si bonds. Hence, the mass loss of GO-NH2 below 650 oC is less than that of GO, in accordance with some reported references [29, 32, 33]. Notably, the insignificant weight loss of GO-NH_2 in the temperature

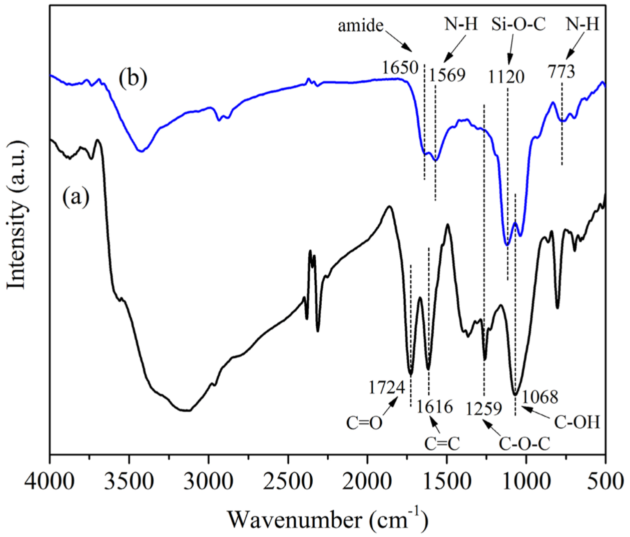

Fig. 1 FT-IR spectra of GO (*a*) and GO-NH_2(*b*)

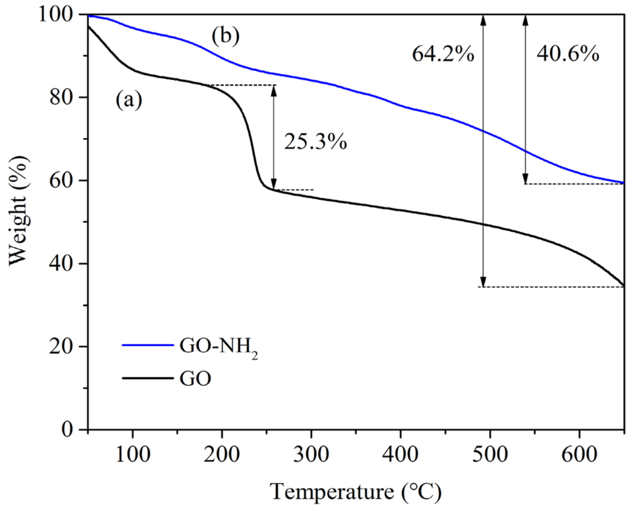

Fig. 2 TG curve of GO (*a*) and GO-NH_2 (*b*)

range of 190–250 °C indicated that a large amount of liable oxygen-containing functional groups, such as C–OH, had been employed to graft APTMS, resulting in the formation of comparatively stable C–O–Si groups. These results indicated the improved thermal stability of GO after grafting with APTMS.

Figure 3 shows the XRD spectra of graphene, GO, and GO-NH_2. The XRD spectrum of graphene exhibited a narrow and strong diffraction peak at about 26.5° attributed to graphene (002). The crystalline interplanar spacing was calculated to be 0.34 nm. However, a new strong characteristic peak at about 12° instead of 26.5° appeared in the XRD spectra of both GO and GO-NH_2, corresponding to graphene oxide (002) [33–35]. A large number of oxygen-containing functional groups produced in the preparation of graphene oxide led to expansion of the graphene layer spacing. Furthermore, a comparatively small 2θ value (11.7°) in the XRD spectrum of GO-NH_2 compared with that of graphene oxide (12.4°) hinted the successful grafting of APTMS on the GO sheets, leading to further expansion of the GO layers. Meanwhile, XRD of the GO modified with different amounts of APTMS are listed in supporting information (Figure S3).

Figure 4a shows only two characteristic peaks for C1s and O1s in the XPS spectrum of GO. However, after grafting APTMS onto GO, two new elements (nitrogen and silicon) derived from APTMS were found in the spectrum (Fig. 4b), indicating the successful synthesis of amine-functionalized GO, in accordance with the FT-IR results. Furthermore, compared with the C1s spectrum of GO (Fig. 4c), that of GO-NH_2 (Fig. 4d) exhibited a new peak for C–O–Si groups (285.6 eV) and a weakened peak for C–OH groups (286.5 eV) [30, 36]. This clearly indicated the covalent combination of APTMS with hydroxyl groups on GO through C–O–Si bonds produced by dealcoholization. Furthermore, weakened peaks for epoxy groups (C–O–C, 287.4 eV) and carboxyl groups (COOH, 288.6 eV) [37] were observed in the C1*s* spectrum of GO-NH_2 (Fig. 4d) compared with those of GO (Fig. 4c). The decrease in epoxy groups on GO-NH_2 might be due to amino groups (–NH_2) on APTMS attacking epoxy groups on GO [13], resulting in the ring opening of epoxy groups for APTMS grafting. Meanwhile, the decreased content of carboxyl groups on GO-NH_2 was attributed to the possible covalent combination of amino groups on APTMS with carboxyl groups on GO during the grafting process, in accordance with FT-IR analysis.

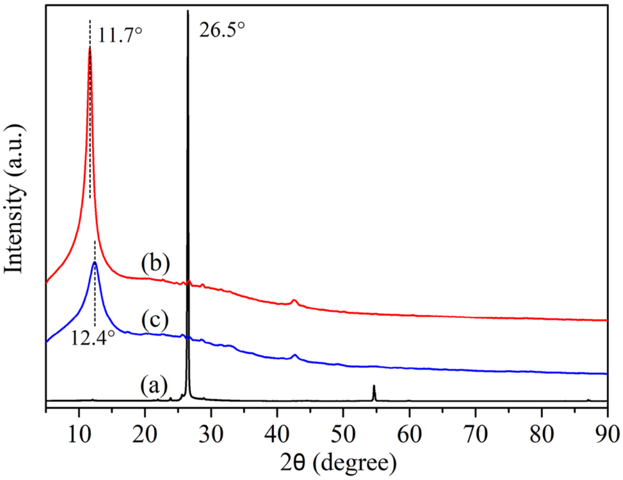

Fig. 3 XRD curve of graphite (*a*), graphite oxide (*b*) and GO-NH_2 (*c*)

In addition, the effects of additive amount of APTMS on amino groups grafted on GO were studied here. OEA analysis of GO-NH_2 samples were summarized in Table S1. Clearly, the more the additive amount of APTMS for grafting, the higher the amino content on GO materials. When additive amount of APTMS reached 2.0 g, the content of amino groups grafted on GO was calculated to be the highest (5.98 mmol/g GO) among 4 samples. Therefore, the sample GO-$NH_2$2.0 was further employed for the following preparation of Pickering emulsion.

3.2 Characterizations of Pickering Emulsion System Prepared by GO-NH_2

The Pickering emulsion system stabilized by GO-NH_2 was observed by optical microscopy. For example, the Pickering emulsion prepared from GO-NH_2 (20 mg), BAL (1.5 mL), and H_2O (4 mL) had a high density of small droplets, as shown in Fig. 5. Droplets in this emulsion had a size distribution of 5–75 μm. According to statistical analysis, droplets with the sizes of 15–20 μm accounted for about 20% of all counted droplets, which was the highest relative frequency in the size distribution. Small droplets with sizes less than 40 μm accounted for about 84% of the total. The mean size of droplets in this Pickering emulsion was calculated to be about 28 μm.

The as-prepared Pickering emulsion was further investigated by comparing its dispersion in water and BAL, respectively. As shown in Fig. 6, the Pickering emulsion stabilized by GO-NH_2 dispersed well in BAL (Fig. 6b), but showed an obvious interface between water and BAL (Fig. 6a). This indicated that the water-in-BAL (W/O) type of Pickering emulsion was stabilized by GO-NH_2, as proven by the smaller contact angle of BAL (about 22°) compared with that of water (about 33°) on the GO-NH_2 surface (Fig. 7) [23, 38].

The surface free energies of GO and GO-NH_2 were further calculated to investigate their wettability. Generally, the higher the surface free energy of a material, the stronger its hydrophilicity. Based on the mathematical model proposed by Owens [39], the surface free energy of a material is composed of dispersion (γ^d) and polar (γ^p) components. The surface free energy (γ_s) of the solid at

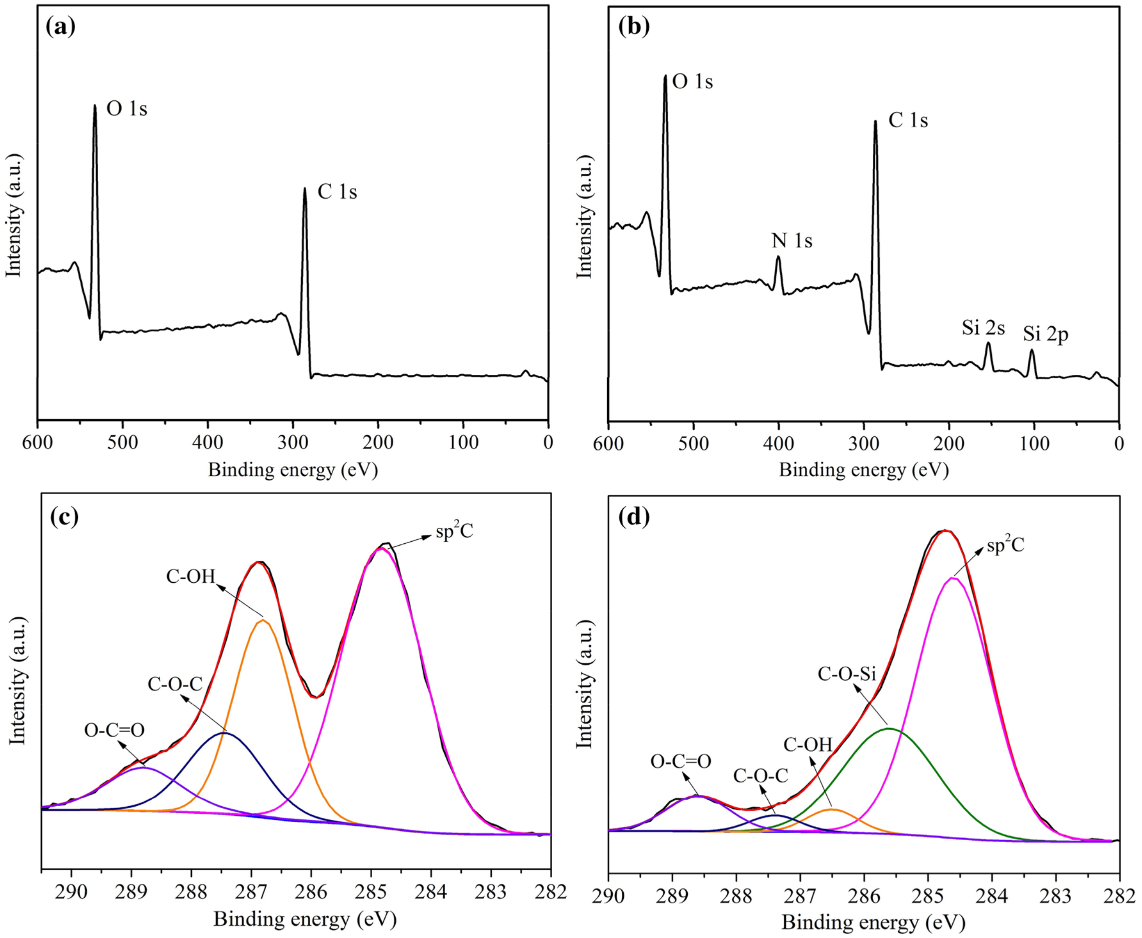

Fig. 4 Survey XPS spectra and C 1*s* ones of GO (**a**, **c**) and GO-NH$_2$ (**b**, **d**)

Fig. 5 Optical micrograph of GO-NH$_2$ stabilized Pickering emulsions

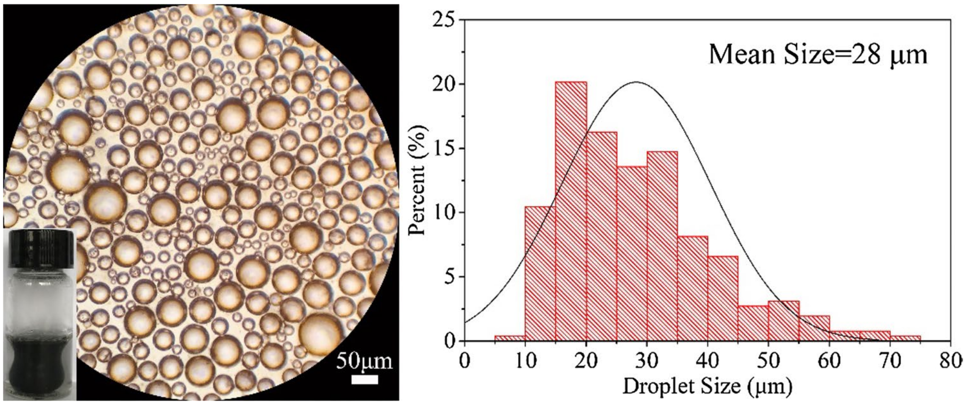

a solid–liquid interface can be calculated from $\gamma_s{}^d + \gamma_s{}^p$, while that of the liquid (γ_l) has a similar expression of $\gamma_l{}^d + \gamma_l{}^p$. In combination with Young's equation, the relationship between surface free energy (γ) and contact angle (θ) can be expressed as shown in Eq. (3).

$$(1 + \cos\theta)\,\gamma_l = 4\left(\gamma_l^d\gamma_s^d/\left(\gamma_l^d + \gamma_s^d\right) + \gamma_l^p\gamma_s^p/\left(\gamma_l^p + \gamma_s^p\right)\right) \quad (3)$$

In this study, water and diiodomethane were employed as test liquids to calculate the surface energy of GO and GO-NH$_2$. Based on the reference [40], dispersion/polar

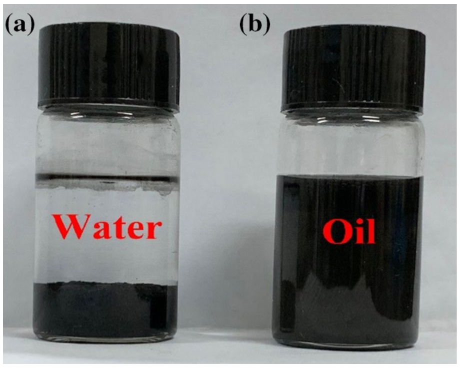

Fig. 6 GO-NH$_2$ stabilized Pickering emulsion dispersion in water (**a**) and benzaldehyde (**b**)

Table 2 Catalytic performance of Pickering emulsion for Knoevenagel condensation

Entry	Catalysts	Conv. (%)	Sel. (%)
1	Blank	25.2	> 99.5
2	GO	32.6	> 99.5
3	SBA-15-NH$_2$	73.7	93.2
4	GO-NH$_2$ stabilized Pickering Emulsion	96.1	> 99.5

Reaction conditions: benzaldehyde (15 mmol), malononitrile (15 mmol), H_2O (4 mL), catalyst (20 mg), n-dodecane (0.3 mL); reaction temperature 50 °C, reaction time 1 h

components (γ_l^d/γ_l^p) of water and diiodomethane are 22.1/50.7 and 44.1/6.7 mJ/m^2, respectively.

Contact angles of water and diiodomethane on both GO and GO-NH$_2$ surfaces were measured, as shown in Figure S1. Thus, surface free energy of GO-NH$_2$ was calculated in Table 1 to be 62.24 mJ/m^2, higher than that of GO (59.40 mJ/m^2). Clearly, the increased surface free energy of GO-NH$_2$ hinted its enhanced hydrophilicity, attributing to the grafting of APTMS on GO. In addition, GO-NH$_2$ surface exhibited small contact angles of water and benzaldehyde (Fig. 7), proving its amphiphilic property.

3.3 Performance of Pickering Emulsion System for Knoevenagel Condensation

The as-prepared Pickering emulsion stabilized by GO-NH$_2$ was further employed in the Knoevenagel condensation, with the results compared with those of GO and APTMS-grafted SBA-15 (SBA-15-NH$_2$), as shown in Table 2. The GO-NH$_2$-stabilized Pickering emulsion exhibited excellent catalytic performance. Using this system, the BAL conversion reached about 96.1% (Table 2, entry 4) at 50 °C in 1 h, which was much higher than those over GO (about 32.6%, entry 2) and SBA-15-NH$_2$ (about 73.7%, entry 3) under the same reaction conditions. Notably, GO itself possesses a few weak basic sites (such as OH and C–O–C groups) on its sheets [41] that result in quite high catalytic activity in the Knoevenagel condensation. However, after grafting APTMS onto GO, the enhancement of strong basic sites (amino groups) on GO-NH$_2$ favored improved catalytic activity

Fig. 7 Contact angles of water (**a**) and BAL (**b**) on GO-NH$_2$ surface

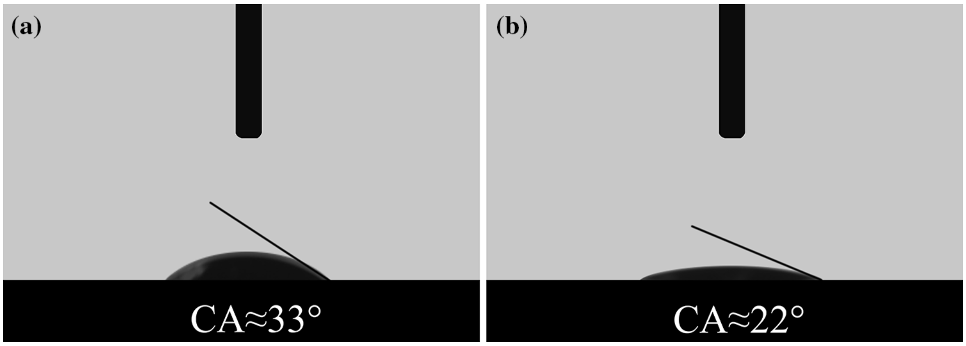

Table 1 The surface wettability of GO and GO-NH$_2$

Catalysts	Contact angle (°)		Surface free energy^{a,b} (mJ/m^2)			
	θ H$_2$O	θ CH$_2$I$_2$	γ	γ^d	γ^p	X^p
GO	37	29	59.40	23.32	36.08	0.61
GO-NH$_2$	33	21	62.24	25.25	36.99	0.59

[a] γ: total surface free energy; $\gamma = \gamma^d + \gamma^p$; γ^d: dispersion component of the surface free energy; γ^p: polar component of the surface free energy; X^p: percentage of the polar component in total surface free energy, γ^p/γ

[b] Surface free energy calculated with the contact angles of the catalysts

in the reaction. In contrast, the greatly decreased OH and C–O–C groups on GO-NH_2 (Fig. 4d) compared with those on GO (Fig. 4c) indicated a minor effect of those groups on the catalytic activity. Therefore, grafted amino groups on GO-NH_2 were an important factor in enhancing catalytic activity toward the Knoevenagel condensation. In contrast, the amphiphilic nature of GO-NH_2 helped with formation of the Pickering emulsion, which showed a high density of small droplets (Fig. 5). As described in Sect. 3.2, the small droplets with sizes of less than 40 μm accounted for about 84% of the total, and the mean droplet size was calculated to be about 28 μm. Therefore, the GO-NH_2-stabilized Pickering emulsion significantly enlarged the interfaces between GO-NH_2 and the reactants, effectively decreasing the mass transfer limitation in the aqueous–organic biphasic system. In contrast, forming a Pickering emulsion with nonamphiphilic SBA-15-NH_2 in the aqueous–organic biphasic system was hard, leading to serious mass transfer limitations in the reaction. Therefore, SBA-15-NH_2 exhibited a lower activity than the GO-NH_2-stabilized Pickering emulsion under the same reaction conditions.

Table 3 Catalytic performance in Knoevenagel condensation over Pickering emulsion and GO-NH_2 in organic solvents

Entry	Medium	Conv. (%)[b]	Sel. (%)
1	GO-NH_2 stabilized Pickering emulsion	96.1	> 99.5
2[a]	THF	78.5	> 99.5
3[a]	Toluene	45.8	> 99.5
4[a]	CH_3CN	33.9	> 99.5
5[a]	$CHCl_3$	31.5	> 99.5
6[a]	CH_2Cl_2	26.6	> 99.5
7[a]	Ethyl acetate	23.8	> 99.5

Reaction conditions: benzaldehyde (15 mmol), malononitrile (15 mmol), solvent (4 mL), catalyst (20 mg), n-dodecane (0.3 mL); reaction temperature 50 °C, reaction time 1 h;

[a] Non-emulsion system

[b] Detailed kinetics data seen in Fig. 9 and Figure S2 (Supporting Information)

3.4 Comparison of Pickering Emulsion and Other Solvents

Table 3 compares the catalytic performance in the Knoevenagel condensation of the Pickering emulsion system and GO-NH_2 in several organic solvents. In nonemulsion catalytic systems, GO-NH_2 achieved the highest catalytic activity in THF among all organic solvents. The BAL conversion into THF was about 78.5% (Table 3, entry 2) after 1 h at 50 °C, which was higher than that in other organic solvents, such as toluene (about 45.8%, entry 3) and ethyl acetate (about 23.8%, entry 7) under the same reaction conditions. This was attributed to the excellent dispersion of GO-NH_2 in THF [42]. The contact angle of THF on GO-NH_2 (Fig. 8f) was measured to be 12°, which was far smaller than those of other solvents, such as ethyl acetate (25°, Fig. 8a) and toluene (17°, Fig. 8e), confirming this opinion. Therefore, the excellent dispersion of GO-NH_2in THF favored the decline of mass transfer limitations in the reaction, resulting in a high activity.

More importantly, compared with nonemulsion catalytic systems, the Pickering emulsion system exhibited a higher activity in the reaction. BAL conversion in the emulsion was 96.1% after 1 h at 50 °C (Table 3, entry 1), while that over GO-NH_2 in THF was only 78.5% under the same reaction conditions. The rate constant, *k*, in the emulsion was further calculated to be 0.043 min^{-1} (Figure 9b), the highest found in this work. This high activity originated from the large interfaces between GO-NH_2 and reactants in the emulsion, as well as the clear confinement effect. Furthermore, as a green solvent, employing water to prepare the Pickering emulsion greatly reduced environmental pollution. Therefore, the Pickering emulsion stabilized by GO-NH_2 showed

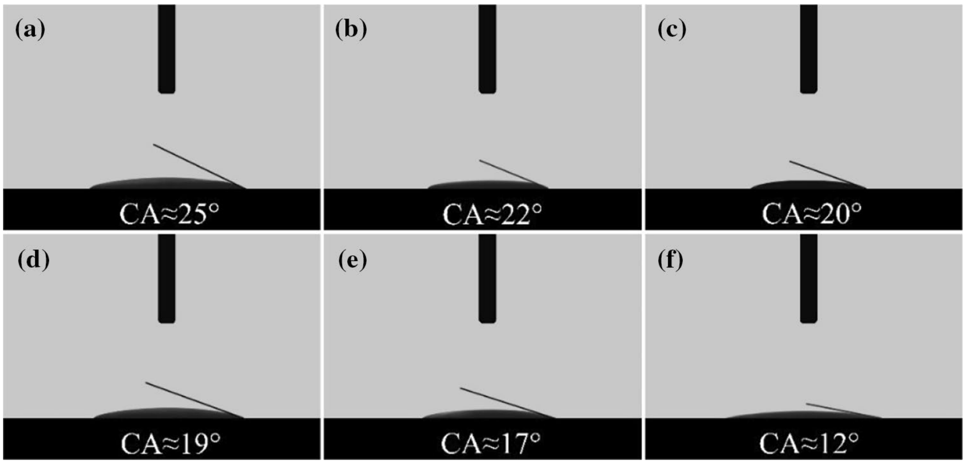

Fig. 8 Contact angles of different organic solvents on GO-NH_2 surface: **a** Ethyl acetate, **b** CH_2Cl_2, **c** $CHCl_3$, **d** CH_3CN, **e** Toluene and **f** THF

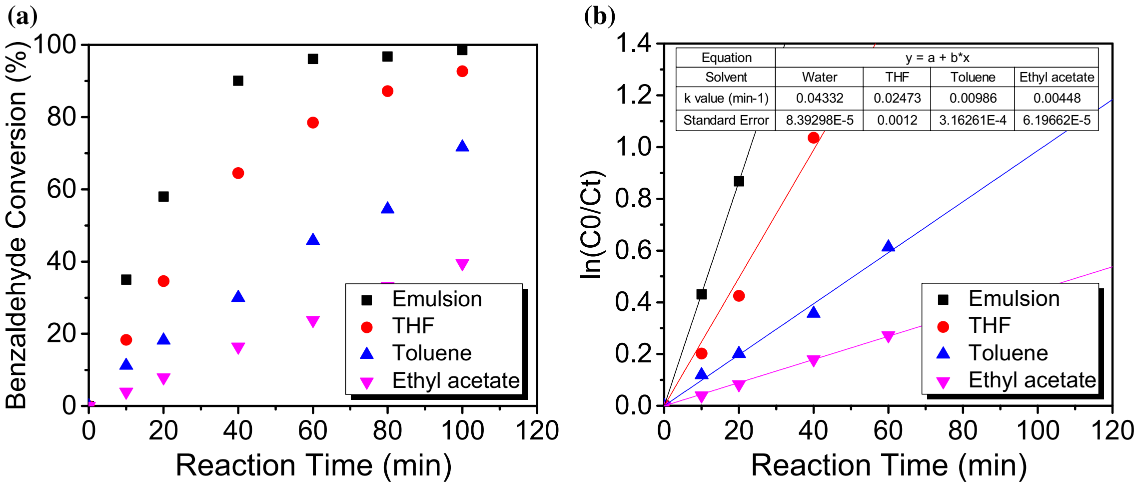

Equation	y = a + b*x			
Solvent	Water	THF	Toluene	Ethyl acetate
k value (min-1)	0.04332	0.02473	0.00986	0.00448
Standard Error	8.39298E-5	0.0012	3.16261E-4	6.19662E-5

Fig. 9 Catalytic activity over GO-NH_2 in several solvents: **a** Benzaldehyde conversion versus reaction time; **b** Reaction rate constants for the reaction

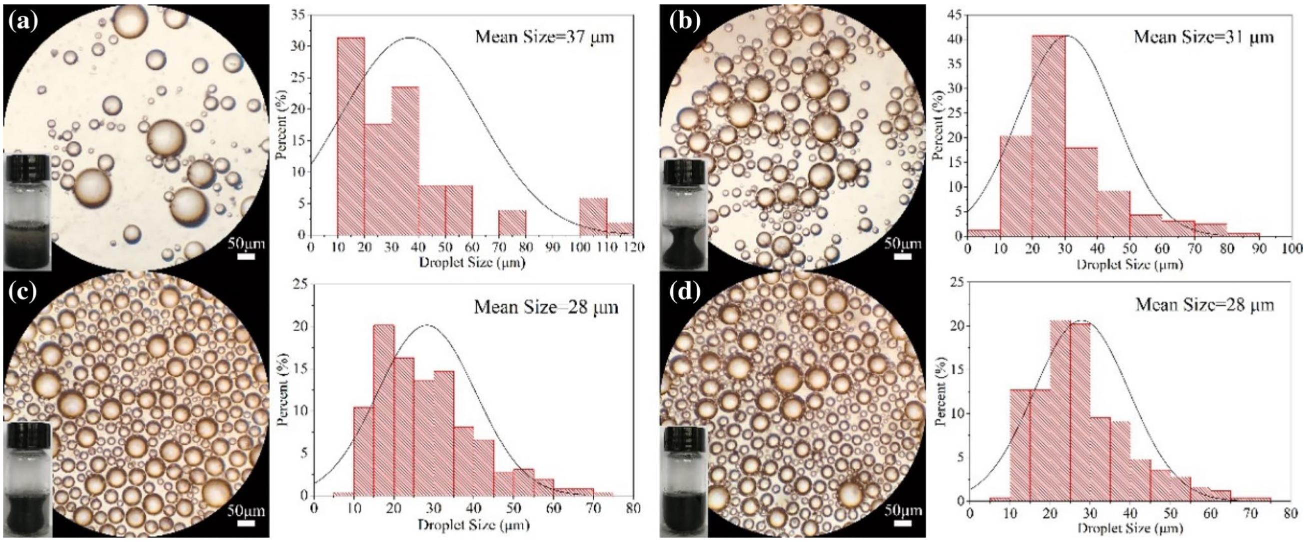

Fig. 10 Optical micrograph of Pickering emulsions prepared using different mass of GO-NH_2 (**a**: 10 mg, **b**: 15 mg, **c**: 20 mg, **d**: 25 mg)

many advantages over the traditional GO-NH_2 catalyst in organic solvents for the Knoevenagel condensation.

3.5 Effect of Emulsion Preparation-Conditions on Its Catalytic Performance

The mass of GO-NH_2 and oil–water ratio greatly affected the properties of the as-prepared Pickering emulsion, including its catalytic performance.

Initially, as shown in Fig. 10, as the mass of GO-NH_2 was increased, the as-prepared emulsion exhibited continuously enhanced catalytic activity. BAL conversion was only 76.8% after 1 h over the sample with 10 mg of GO-NH_2 (Table 4, entry 2), but climbed to 96% when the mass of GO-NH_2

Table 4 Catalytic performance in Knoevenagel condensation over Pickering emulsions prepared using different amount of GO-NH_2

Entry	Catalyst weight (mg)	Conv. (%)	Sel. (%)
1	Blank	25.2	> 99.5
2	10	76.8	> 99.5
3	15	82.9	> 99.5
4	20	96.1	> 99.5
5	25	99.0	> 99.5

Pickering emulsion system was composed of benzaldehyde (15 mmol), malononitrile (15 mmol), H_2O (4 mL), n-dodecane (0.3 mL) and GO-NH_2 (10–25 mg); Reaction conditions: 50 °C for 1 h was increased to 20 mg (entry 4). The high activity of this Pickering emulsion system was strongly correlated with its excellent properties. For instance, the sample with 10 mg of GO-NH_2 (Fig. 10a) had comparatively large droplets with a low density. Droplets in this emulsion had a size distribution of 10–120 μm in width. Based on statistical analysis, small droplets with sizes of less than 40 μm accounted for about 71% of all droplets counted. Meanwhile, a certain number of large droplets with sizes above 100 μm were also discovered in this emulsion, accounting for about 8% of the total droplets. The mean size was calculated to be about 37 μm. Therefore, comparatively small interfaces between GO-NH_2 and reactants in this emulsion led to low catalytic activity in the reaction. In contrast, when the mass of GO-NH_2 reached 20 mg, the prepared Pickering emulsion exhibited enhanced properties. A high density of small droplets was observed in this emulsion through optical microscopy (Fig. 10c). Droplets in this emulsion exhibited a size distribution of 5–75 μm. Those with small sizes less than 40 μm accounted for about 84% of the total, which was much higher than the sample with 10 mg of GO-NH_2. Meanwhile, no droplets with large sizes above 80 μm were found in this emulsion. The mean droplet size was further calculated to be about 28 μm. This emulsion had comparatively large interfaces between GO-NH_2 and the reactants, which helped enhance the catalytic activity. When the mass of the catalyst was beyond 20 mg, the unchanged emulsion properties (Fig. 10c, d) led to a slight increase in conversion from about 96% to 99% (Table 4, entry 5). Therefore, the Pickering emulsion prepared from 20 mg of GO-NH_2 possessed high catalytic efficiency in the reaction. Furthermore, all samples possessed high selectivity toward benzylidenemalononitrile (> 99.5%), which was beneficial to product purification after the reaction.

Table 5 Catalytic performance in Knoevenagel condensation over Pickering emulsions prepared using different amount of water

Entry	*V* (mL)	Conv. (%)	Sel. (%)
1	3	87.0	> 99.5
2	4	96.1	> 99.5
3	5	86.8	> 99.5
4	6	83.2	> 99.5

Pickering emulsion system was composed of benzaldehyde (15 mmol), malononitrile (15 mmol), H_2O (3–6 mL), n-dodecane (0.3 mL) and GO-NH_2 (20 mg); Reaction conditions: 50 °C for 1 h

Furthermore, the effect of the oil–water ratio on emulsion formation and catalytic activity was investigated. When the amount of water added reached 4 mL, the prepared emulsion exhibited the highest BAL conversion among all samples (about 96%; Table 5, entry 2) owing to its excellent properties (Fig. 11b). In contrast, three other samples exhibited comparatively low activities in the reaction owing to their low densities of large droplets. For example, the sample with 6 mL of water (entry 4) had the lowest BAL conversion of about 83%, which was about 13% lower than that with 4 mL of water. Droplets in this emulsion exhibited a wide-ranging size distribution of 20–200 μm. The small droplets with sizes less than 40 μm only accounted for about 16% of the total, which was far lower than that of the sample with 4 mL of water (about 84% of the total, Fig. 11b). Meanwhile, a number of large droplets with sizes above 100 μm were discovered in this emulsion, accounting for about 15% of the total. The mean size was calculated to be about 67 μm.

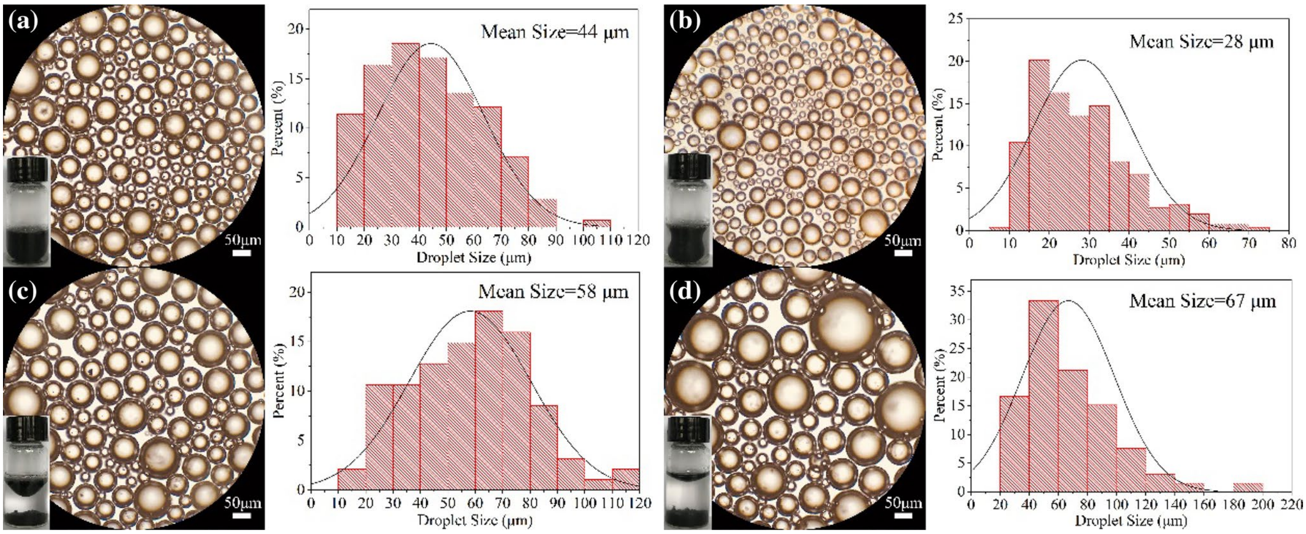

Fig. 11 Optical micrograph of Pickering emulsions prepared using 3 mL (**a**), 4 mL (**b**), 5 mL (**c**) and 6 mL (**d**) of water and size distributions of droplets in them

Logically, the large sizes of droplets in the emulsion shrank the interfaces between GO-NH_2 and reactants, leading to the comparatively low catalytic activity.

In summary, the Pickering emulsion prepared from GO-NH_2 (20 mg) and H_2O (4 mL) possessed the smallest droplets with the highest density. This emulsion exhibited comparatively large interfaces between GO-NH_2 and BAL for the reaction, resulting in a high catalytic activity and was, therefore, used for subsequent reactions.

3.6 Exploration of Substrates Scope

To explore the substrate scope of the GO-NH_2-based Pickering emulsion, several aldehydes, including aromatic aldehydes with electron-withdrawing groups (Table 6, entries 1 and 2) and electron-donating groups (entries 3 and 4), a heterocyclic aldehyde (entry 5), and a long-chain aliphatic aldehyde (entry 6) were employed for the Knoevenagel condensation with malononitrile in this catalytic system. The results showed that the GO-NH_2-stabilized emulsion produced a high density of small droplets, which greatly enlarged interfaces between GO-NH_2 and the reactants. Therefore, the Pickering emulsion overcame mass transfer limitations between oil–water interfaces, efficiently enhancing the catalytic activity of active sites on GO-NH_2, as proven by the high conversions of aldehydes in the Pickering emulsion catalytic system (Table 6). Furthermore, compared with substrates bearing electron-donating groups, such as *p*-tolualdehyde (entry 3) and *p*-methoxybenzaldehyde (entry 4), those with electron-withdrawing groups, such as 2-fluorobenzaldehyde (entry 1) and *p*-fluorobenzaldehyde (entry 2), achieved a slightly higher conversion. This was attributed to strong electron-positive carbonyl carbon in the compound with electron-withdrawing groups facilitating the attack of carbanions of active methylene compounds, such as malononitrile. Furthermore, the Pickering emulsion had a higher catalytic activity toward aromatic aldehydes as substrates than aliphatic aldehydes. For example, the *p*-tolualdehyde conversion over the Pickering emulsion reached 98.2% in 1 h

Table 6 Catalytic performance in Knoevenagel condensation over Pickering emulsions prepared using several aldehydes

Entry	Aldehyde	Nitrile	Conv. (%)	Sel. (%)
1	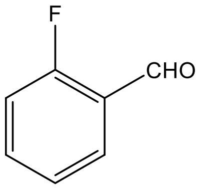	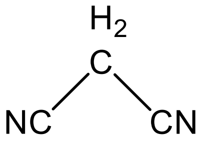	99.1	> 99.5
2	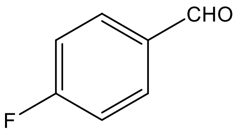	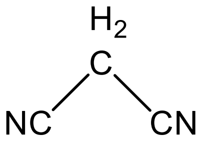	98.6	> 99.5
3	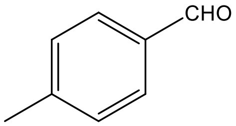	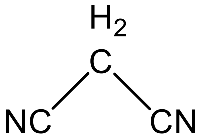	98.2	> 99.5
4	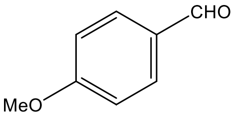	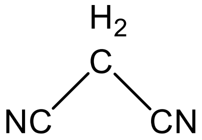	95.8	> 99.5
5	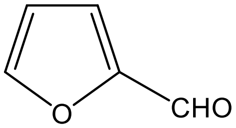	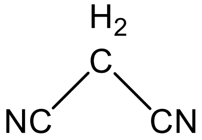	89.1	> 99.5
6	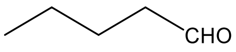	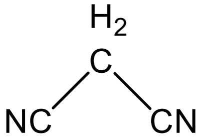	85.2	98.6

Pickering emulsion system was composed of aldehyde (15 mmol), malononitrile (15 mmol), H_2O (4 mL), n-dodecane (0.3 mL) and GO-NH_2 (20 mg); Reaction conditions: 50 °C for 1 h (entry 3), which was 13% higher than that of valeraldehyde (entry 6). The high conversions of aromatic aldehydes over the catalytic system were possibly due to the strong interaction between aromatic rings and GO. This aided formation of the Pickering emulsion possessing a high density of droplets in the aqueous phase.

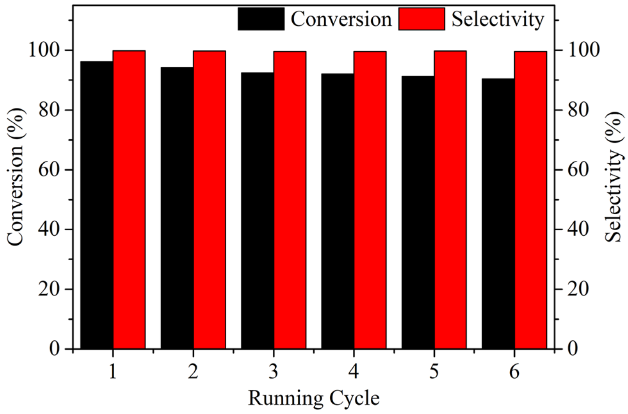

Fig. 12 Recycling of GO-NH_2 across 6 running cycles

3.7 Catalyst Recycling

Finally, the reusability of catalyst GO-NH_2 was examined owing to its heterogeneous nature. The results showed that GO-NH_2 maintained high activity across six runs. The BAL conversion slightly declined from about 96% to 90% (Fig. 12), which was mainly ascribed to some mass loss of the catalyst during recycling. The properties of recycled GO-NH_2 were further studied by optical microscope, XRD, FT-IR and XPS. XRD spectrum of recycled GO-NH_2 (Fig. 13a) exhibited the characteristic peak at about 12° on behalf of GO (002), similar to that of fresh one. Its FT-IR spectrum (Fig. 13b) and XPS ones (Fig. 13c, d) hinted the presence of C-O-Si groups, proving the stability of GO-NH_2. The Pickering emulsion after 6 runs exhibited good properties as well (Fig. 14). Droplets in this emulsion exhibited the size distribution in the range of 10–90 µm (Fig. 14). Those with small sizes less than 40 µm accounted for about 80% of the total. The mean size of droplets in this Pickering emulsion was about 32 µm. In summary, the synthesized GO-NH_2 in this work had good recyclability and reusability.

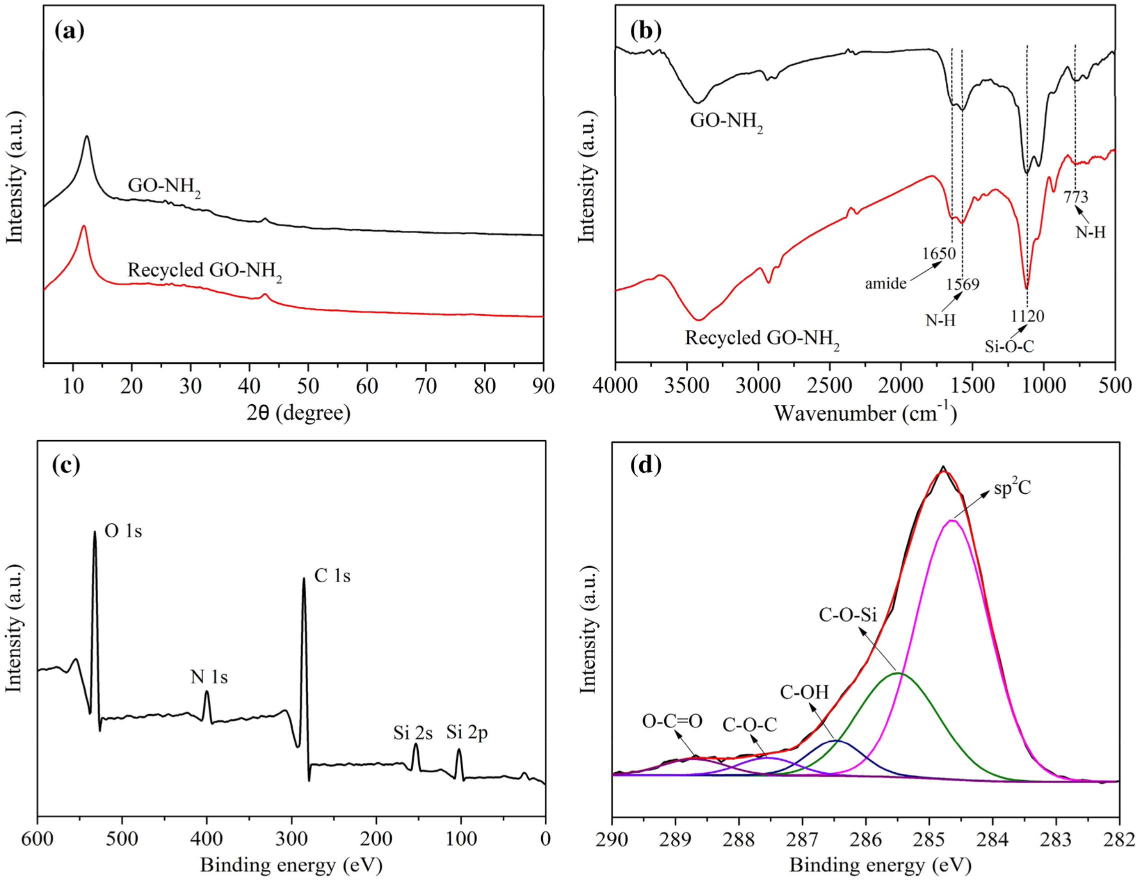

Fig. 13 XRD (**a**), FT-IR (**b**), XPS survey (**c**) and C 1*s* (**d**) spectra of GO-NH_2 after 6 runs

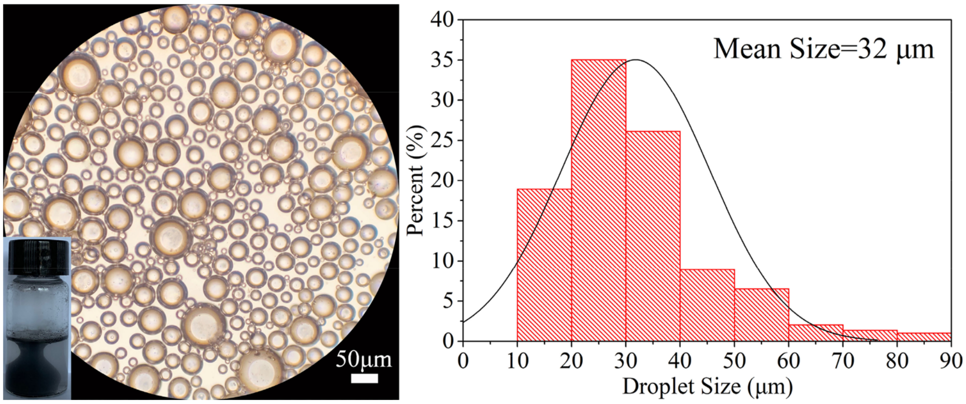

Fig. 14 Optical micrograph of Pickering emulsion after 6 runs

4 Conclusions

An amphiphilic amine-functionalized graphene oxide (GO-NH_2) was successfully synthesized for the preparation of a W/O-type Pickering emulsion. This Pickering emulsion achieved high catalytic activity in the aqueous Knoevenagel condensation under a mild reaction temperature for a short time owing to its large interfaces between catalysts and reactants, and the confinement effect in the Pickering emulsion. GO-NH_2 showed excellent recyclability and reusability. Pickering emulsions prepared using amphiphilic GO-based materials have broad application prospects in heterogeneous interfacial catalysis.

Acknowledgements This work was supported by the National Natural Science Foundation of China (No. 21673024 and No. 21676029). The financial support from the Priority Academic Program Development of Jiangsu Higher Education Institutions (PAPD) is also acknowledged.

References

1. Saravanamurugan S, Palanichamy M, Hartmann M, Murugesan V (2006) Appl Catal A 298:8–15
2. Zhang X, Lai ESM, Martin-Aranda R, Yeung KL (2004) Appl Catal A 261:109–118
3. Chen X, Arruebo M, Yeung KL (2013) Catal Today 204:140–147
4. Ansari MB, Jin H, Parvin MN, Park S-E (2012) Catal Today 185:211–216
5. Dalessandro EV, Collin HP, Guimarães LGL, Valle MS, Pliego JR (2017) J Phys Chem B 212:5300–5307
6. Li X, Lin B, Li H, Yu Q, Ge Y, Jin X, Liu X, Zhou Y, Xiao J (2018) Appl Catal B 239:254–259
7. Kan-nari N, Okamura S, Fujita S, Ozaki J, Arai M (2010) Adv Synth Catal 352:1476–1484
8. Zheng L, Li P, Tao M, Zhang W (2019) Catal Commun 118:19–24
9. Zhu F, Sun X, Lou F, An L, Zhao P (2015) Catal Lett 145:1072–1079
10. Wang S-G (2003) Catal Commun 4:469–470
11. Angeletti E, Canepa C, Martinetti G, Venturello P (1988) Tetrahedron Lett 29:2261–2264
12. Parida KM, Mallick S, Sahoo PC, Rana SK (2010) Appl Catal A 381:226–232
13. Xue B, Zhu J, Liu N, Li Y (2015) Catal Commun 64:105–109
14. Li G, Xiao J, Zhang W (2011) Green Chem 13:1828–1836
15. Tobiszewsk M, Tsakovsk S, Simeonov V, Namieśnik J, Pena-Pereira F (2015) Green Chem 17:4773–4785
16. Wei L, Zhang M, Zhang X, Xin H, Yang H (2016) ACS Sustain Chem Eng 4:6838–6843
17. Xue F, Zhang Y, Zhang F, Ren X, Yang H (2017) ACS Appl Mater Interfaces 9:8403–8412
18. Huang J, Yang H (2015) Chem Commun 51:7333–7336
19. Yang H, Fu L, Wei L, Liang J, Binks BP (2015) J Am Chem Soc 137:1362–1371
20. Zapata PA, Faria J, Ruiz MP, Jentoft RE, Resasco DE (2012) J Am Chem Soc 134:8570–8578
21. Wang Y, Rong Z, Wang Y, Qu J (2016) J Catal 333:8–16
22. Sun Z, Rong Z, Wang Y, Xia Y, Du W, Wang Y (2014) RSC Adv 4:1874–1878
23. Zhang F, Jiang H, Li X, Wu X, Li H (2014) ACS Catal 4:394–401
24. Luo Q, Wang Y, Yoo E, Wei P, Pentzer E (2018) Langmuir 34:10114–10122
25. He Y, Wu F, Sun X, Li R, Guo Y, Li C, Zhang L, Xing F, Wang W, Gao J (2013) ACS Appl Mater Interfaces 5:4843–4855
26. Marcano DC, Kosynkin DV, Berlin JM, Sinitskii A, Sun ZZ, Slesarev A, Alemany LB, Lu W, Tour JM (2010) ACS Nano 4:4806–4814
27. Burrell MC, Armstrong NR (1983) Appl Surf Sci 17:53–69
28. Liu F, Sun J, Zhu L, Meng X, Qi C, Xiao F-S (2012) J Mater Chem 22:5495–5502
29. Valentini L, Bon SB, Monticell O, Kenny JM (2012) J Mater Chem 22:6213–6217
30. Chong ASM, Zhao XS (2003) J Phys Chem B 107:12650–12657
31. Yang H, Li F, Shan C, Han D, Zhang Q, Niu L, Ivaska A (2009) J Mater Chem 19:4632–4638
32. Matsuo Y, Nishino Y, Fukutsuka T, Sugie Y (2007) Carbon 45:1384–1390
33. Huang J, Ding S, Xiao W, Peng Y, Deng S, Zhang N (2015) Catal Lett 145:1000–1007
34. Wu T, Wang X, Qiu H, Gao J, Wang W, Liu Y (2012) J Mater Chem 22:4772–4779
35. Li Y, Gao W, Ci L, Wang C, Ajayan PM (2010) Carbon 48:1124–1130
36. Pokhrela J, Bhoriaa N, Anastasioua S, Tsoufis T, Gournisc D, Romanos G, Karanikolos GN (2018) Microporous Mesoporous Mater 267:53–67
37. Ramanathan T, Fisher FT, Ruoff RS, Brinson LC (2005) Chem Mater 17:1290–1295
38. Wan Y-J, Tang L-C, Gong L-X, Yan D, Li Y-B, Wu L-B, Jiang J-X, Lai G-Q (2014) Carbon 69:467–480
39. Owens DK, Wendt RC (1969) J Appl Polym Sci 13:1741–1747

40. Su ZF, Zuo BQ (2011) Silk 48:13–15
41. Islam SM, Roy AS, Dey RC, Paul S (2014) J Mol Catal A 394:66–73
42. Paredes JI, Villar-Rodil S, Martínez-Alonso A, Tascón JMD (2008) Langmuir 24:10560–10564

Affiliations

Jie Zhu[1] · Fei Wang[1] · Dongsheng Li[1] · Jie Zhai[1] · Ping Liu[1] · Weihong Zhang[1] · Yongxin Li[1]

✉ Yongxin Li
liyxluck@163.com

[1] Jiangsu Key Laboratory of Advanced Catalytic Materials
and Technology, School of Petrochemical Engineering,
Changzhou University, Changzhou 213164, China